J Bioenerg Biomembr (2010) 42:1–10
DOI 10.1007/s10863-009-9266-y

The effect of NBD-Cl in nucleotide-binding of the major subunit α and B of the motor proteins F_1F_O ATP synthase and A_1A_O ATP synthase

Cornelia Hunke · Vikeramjeet Singh Tadwal · Malathy Sony Subramanian Manimekalai · Manfred Roessle · Gerhard Grüber

Received: 20 October 2009 / Accepted: 10 December 2009 / Published online: 16 January 2010

Abstract Subunit α of the *Escherichia coli* F_1F_O ATP synthase has been produced, and its low-resolution structure has been determined. The monodispersity of α allowed the studies of nucleotide-binding and inhibitory effect of 4-Chloro-7-nitrobenzofurazan (NBD-Cl) to ATP/ADP-binding. Binding constants (K_d) of 1.6 μM of bound MgATP-ATTO-647N and 2.9 μM of MgADP-ATTO-647N have been determined from fluorescence correlation spectroscopy data. A concentration of 51 μM and 55 μM of NBD-Cl dropped the MgATP-ATTO-647N and MgADP-ATTO-647N binding capacity to 50% (IC_{50}), respectively. In contrast, no effect was observed in the presence of *N,N′*-dicyclohexylcarbodiimide. As subunit α is the homologue of subunit B of the A_1A_O ATP synthase, the interaction of NBD-Cl with B of the A-ATP synthase from *Methanosarcina mazei* Gö1 has also been shown. The data reveal a reduction of nucleotide-binding of B due to NBD-Cl, resulting in IC_{50} values of 41 μM and 42 μM for MgATP-ATTO-647N and MgADP-ATTO-647N, respectively.

Keywords F_1F_O ATP synthase · A_1A_O ATP synthase · Subunit α · Subunit B · 4-Chloro-7-nitrobenzofurazan (NBD-Cl) · *N,N′*-dicyclohexylcarbodiimide (DCCD) · Small angle X-ray scattering (SAXS) · Fluorescence correlation spectroscopy (FCS)

Abbreveations

CD	circular dichroism
Cy5	Cyanine 5
DTT	dithiothreitol
DCCD	N,N′-dicyclohexylcarbodiimide
FCS	fluorescence correlation spectroscopy
IPTG	isopropyl-β-D-thiogalactopyranoside
NBD-Cl	4-Chlor-7-nitrobenzofurazan
NTA	nitrilotriacetic acid
PAGE	polyacrylamide gel electrophoresis
PCR	polymerase chain reaction
PMSF	phenylmethylsulphonyl fluoride
SAXS	small angle X-ray scattering
SDS	sodium dodecyl sulfate
Tris	Tris-(hydroxymethyl)aminomethane

Introduction

The adenosine triphosphate (ATP) molecule is the common energy source of biological cells. When cells require energy, they hydrolyze ATP to adenosine diphosphate (ADP) and inorganic phosphate (P_i). The enzymes respon-

Authors Cornelia Hunke and Vikeramjeet Singh Tadwal have equal contribution.

Electronic supplementary material The online version of this article (doi:10.1007/s10863-009-9266-y) contains supplementary material, which is available to authorized users.

C. Hunke · V. S. Tadwal · M. S. S. Manimekalai · G. Grüber (✉)
School of Biological Sciences,
Nanyang Technological University,
Singapore 637551, Republic of Singapore
e-mail: ggrueber@ntu.edu.sg

M. Roessle
European Molecular Biology Laboratory, Hamburg Outstation,
EMBL c/o DESY,
22603 Hamburg, Germany

G. Grüber
Bioinformatics Institute (A*STAR),
30 Biopolis Street, #07-01 Matrix,
Singapore 138671, Republic of Singapore

sible for the generation of ATP inside eukaryotic and prokaryotic cells are the so-called F_1F_O ATP synthases (F-ATP synthases). F-ATP synthases use an ion electrochemical gradient, consisting of a voltage and a pH gradient across membranes of cristae and thylakoids, to synthesize ATP in mitochondria and chloroplasts, respectively. The same mechanisms are used by the F-ATP synthase of prokaryotes. Unlike energy conservation mechanism in eukaryotes and prokaryotes, energy conservation in archaea, like methanogens, is coupled to the generation of a H^+- and Na^+-gradient across the membrane, at which both ion gradients are believed to drive synthesis of ATP in them (Deppenmeier and Müller 2008). The mechanism of coupling between ATP production, catalyzed by the A_1A_O ATP synthase (A-ATP synthase), and the two ion gradients is largely unknown. The membrane-integrated enzyme is composed of ten subunits. Both the A-ATP synthase as well as the bacterial F-ATP synthase are divided into a water soluble A_1 and F_1 sector, comprised of the subunits A_3:B_3:C:D:E_x:F:G:H_2 and α_3:β_3:γ:δ:ε, respectively, and an integral membrane A_O and F_O domain, which is involved in ion translocation, and made-up by the subunits *a*:c_x and *a*:*b*:c_x, respectively (Lolkema et al. 2003; Pedersen et al. 2000; Grüber and Marshansky 2008; Cross and Müller 2004). The major nucleotide-binding subunits A and B of the A_1 and the corresponding β and α subunits of the F_1 domain display the highest degree of sequence similarity with an overall identity of approximately 25% (Nelson 1992). The major difference between the A subunits of the A-ATP synthases and the β subunit of F-ATP synthases is caused by the so-called "nonhomologous region", an insertion of about 90 amino acids near the N-terminus of subunit A (Nelson 1992; Hilario and Gogarten 1998). The non-catalytic B subunits of the A-ATP synthases/V-ATPases do not have the consensus sequence (GXXGXGKTV), called phosphate binding loop (P-loop), although it is able to bind nucleotides (Schäfer et al. 2006). It has been shown that the A and B subunits of A_1 and the α and β subunits of F_1 form an alternating hexagonal arrangement around a central stalk (Coskun et al. 2004a,b; Vonck et al. 2009; Hausrath et al. 1999; Leslie and Walker 2000; Walker and Dickson 2006). The pseudohexameric headpiece is attached to the A_O/F_O part by the central stalk and by one or more peripheral stalk(s) (Lolkema et al. 2003; Grüber and Marshansky 2008; Vonck et al. 2009; Coskun et al. 2004a,b; Bernal and Stock 2004).

As these enzyme complexes represent the class of biological energy producers, a variety of ions, natural products and covalent effectors have been analyzed, which bind to specific sites of the catalytic F_1 domain (Gledhill and Walker 2006; Hong and Pedersen 2008). The covalent inhibitors include 4-Chloro-7-nitrobenzofurazan (NBD-Cl) and *N,N′*-dicyclohexylcarbodiimide (DCCD). NBD-Cl is a fluorescent adenine analog that labels Tyr or Lys residues and inhibits the processes of ATP synthesis as well as hydrolysis (Andrews et al. 1984a,b; Sutton and Ferguson 1985; Haughton and Capaldi 1995). The crystallographic structure of the bovine F_1 ATPase reveals the NBD-Cl molecule at the open α_E-β_E interface with the modified Y311 of nucleotide empty subunit β (β_E) and the residues V334, S335, T340, I343 and F351 of the α_E subunit as well as residues V312, P313, A314 and D315 of β_E, forming the NBD-Cl-binding pocket ((Orriss et al. 1998), Fig. 1a). NBD-Cl appears to inhibit F_1 by preventing β_E from undergoing a conformational change (Orriss et al. 1998). Like NBD-Cl, only one molecule of DCCD reacts with the bovine F_1 ATPase, which is associated with residue E199 in

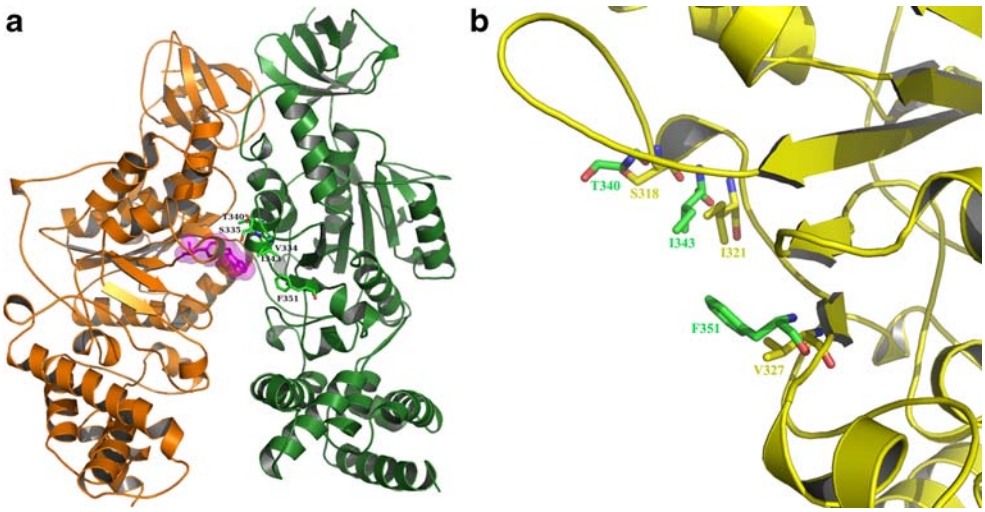

Fig. 1 Amino acid residues forming the NBD-Cl binding pocket. (**a**) The important amino acid residues that are found to form the NBD-Cl binding region in the bovine F_1 ATPase (1NBM (Orriss et al. 1998)). (**b**) The amino acids, comprising the NBD pocket of subunit α (*green*) compared with the homologue residues (*yellow*) in the crystallographic structure of wild type B subunit of *M. mazei* Gö1 (2C61 (Schäfer et al. 2006))

the ADP occupied β subunit, β_{DP} (Gibbons et al. 2000). The DCCD-binding pocket was found to be in the α_{DP}-β_{DP} interface, with the residues V164, M167, V420 and F424 contributing to this side. It is proposed that DCCD-binding causes a steric hindrance and blocks a conformational change from β_{DP} to β_E. So far the focus of inhibitory effect (s) of both effectors was mostly oriented towards the catalytic β subunit although the binding pockets of NBD-Cl and DCCD are in the α-β interface. Here we focused our attention on the possible effect of nucleotide-binding of subunit α of the *E. coli* F_1F_O ATP synthase by the presence of these both effectors, preparing a monodisperse protein and providing insight into the involvement of NBD-Cl inhibition in nucleotide-binding of subunit α. In parallel, fluorescence correlation spectroscopy (FCS) studies revealed that ATP as well as ADP binding to subunit B of the related A-ATP synthase becomes inhibited by NBD-Cl, whereby no effect could be detected in the presence of DCCD.

Experimental procedures

Biochemicals

PROOFSTART DNA Polymerase and Ni^{2+}-NTA-chromatography resin were received from Qiagen (Hilden, Germany); restriction enzymes were purchased from Fermentas (St. Leon-Rot, Germany). Chemicals for gel electrophoresis were received from Serva (Heidelberg, Germany). Bovine serum albumin was purchased from GERBU Biochemicals (Heidelberg, Germany). The ATP- and ADP-analogues EDA-ATP ATTO-647N and EDA-ADP ATTO-647N were received from ATTO-TEC (Siegen, Germany). All other chemicals were at least of analytical grade and received from BIOMOL (Hamburg, Germany), Merck (Darmstadt, Germany), Roth (Karlsruhe, Germany), Sigma (Deisenhofen, Germany), or Serva (Heidelberg, Germany).

Production and purification of subunit α and B

To amplify *atp*A, encoding the gene of the nucleotide-binding subunit α of the *EC*F_1F_O ATP synthase, the oligonucleotide primers 5′-CCT GTT CAC CAT GGC TTG CA-3′ (forward primer) and the same reverse primer 5′ CCC GAG CTC CTT ACA GTT CAG 3′, incorporating *Nco*I and *Sac*I restriction sites (underlined), were designed. The *unc* containing plasmid pGG1 (Grüber and Capaldi 1996) was used as the template for polymerase chain reaction (PCR). Following digestion with *Nco*I and *Sac*I, the PCR products were ligated into the pET9d1-His_3 vector (Grüber et al. 2002). The pET9d1-His_3 vector, containing the gene *atp*A was then transformed into *E. coli* cells (strain BL21 (DE3)) and grown on 30 μg/ml kanamycin-containing Luria-Bertoni (LB) agar-plates. To produce the protein, liquid cultures were shaken in LB medium containing kanamycin (30 μg/ml) for about 6 h at 37 °C until an optical density OD_{600} of 0.6–0.7 was reached. To induce the production of His_3-α the culture was supplemented with isopropyl-β-D-thiogalactopyranoside (IPTG) to a final concentration of 1 mM. Following incubation for another 4 h at 37 °C, the cells were harvested at 10,000×*g* for 15 min, 4 °C. Subsequently, they were lysed on ice by sonication for 3×1 min in buffer A (50 mM Tris/HCl, pH 7.5, 200 mM NaCl, 1 mM DTT, 1 mM PMSF). The lysate was cleared by centrifugation at 10,000×*g* for 35 min, 4 °C. The supernatant was filtered (0.45 μm; Millipore) and incubated with Ni^{2+}-NTA resin. The His-tagged protein was allowed to bind to the matrix for 2 h at 4 °C and was eluted with an imidazole-gradient (25–300 mM) in buffer A. Fractions containing His_3-tagged protein were identified by SDS-PAGE, (Laemmli 1970) pooled and concentrated as required using Centricon YM-30 (30 kDa molecular mass cut off) spin concentrators (Millipore). In a second chromatographic step, the concentrated sample was loaded onto a gel filtration column (Superdex 75 HR 10/30 column, GE Healthcare) and the protein was eluted using buffer B (50 mM Tris/HCl, pH 7.5 and 200 mM NaCl). Subunit B of the A_1A_O ATP synthase from *Methanosarcina mazei* Gö1 was isolated as described previously (Schäfer et al. 2006). The purity of all protein samples were analyzed by SDS-PAGE. SDS-gels were stained with Coomassie Brilliant Blue G250. Protein concentrations were determined by the bicinchoninic acid assay (BCA; Pierce, Rockford, IL. USA).

Circular dichroism spectroscopy

Steady state CD spectra were measured in the far UV-light (185–260 nm) using a CHIRASCAN spectropolarimeter (Applied Photophysics). Spectra were collected in a 60 μl quartz cell (Hellma) with a path length of 0.1 mm, at 20 °C and a step resolution of 1 nm. The readings were average of 2 s at each wavelength and the recorded ellipticity values were the average of three determinations for each sample. CD spectroscopy of subunit α (2 mg/ml) was performed in a buffer of 50 mM Tris/HCl (pH 7.5) and 200 mM NaCl. The spectrum for the buffer was subtracted from the spectrum of the protein. CD values were converted to mean residue ellipticity (Θ) in units of degree cm^2 $dmol^{-1}$ using the software Chirascan Version 1.2, Applied Photophysics. This baseline corrected spectrum was used as input for computer methods to obtain predictions of secondary structure. The CD spectra were analyzed as described recently (Biuković et al. 2007).

X-ray scattering experiments and data analysis

The synchrotron radiation X-ray scattering data were collected following standard procedures on the X33 SAXS camera (Boulin et al. 1986) of the EMBL Hamburg located on a bending magnet (sector D) on the storage ring DORIS III of the Deutsches Elektronen Synchrotron (DESY). A photon counting Pilatus 1M pixel detector (67×420 mm^2) was used (Roessle et al. 2007) at a sample-detector distance of 2.4 m covering the range of momentum transfer $0.1<s<4.5$ nm^{-1} ($s=4$ p $\sin(q)/l$, where q is the scattering angle and $l=0.15$ nm is the X-ray wavelength). The S-axis was calibrated by the scattering pattern of Silver-behenate salt (d-spacing 5.84 nm). The scattering patterns from subunit α were measured at protein concentrations of 2.0 and 8.0 mg/ml, respectively. Protein samples were prepared in 50 mM Tris/HCl (pH7.5), 200 mM NaCl and 1.25 mM DTT as radical quencher and injected automatically using the sample-changing robot for solution scattering experiments at the SAXS station X33 (Round et al. 2008). The data were normalized to the intensity of the incident beam; the scattering of the buffer was subtracted and the difference curves were scaled for concentration. All the data processing steps were performed using the program package PRIMUS (Svergun 1993). The forward scattering *I(0) and the radius of gyration R_g were evaluated using the Guinier approximation (Guinier and Fournet 1955).*

The molecular mass of subunit α was calculated by comparison with the forward scattering from the reference solution of bovine serum albumin (BSA). From this procedure a relative calibration factor for the molecular mass (MM) can be calculated using the known molecular mass of BSA (66 kDa) and the concentration of the reference solution by applying

$$MM_p = I(0)_p/c_p \times \frac{MM_{st}}{I(0)_{st}/c_{st}}$$

where $I(0)_p$, $I(0)_{st}$ are the scattering intensities at zero angle of the studied and the BSA standard protein, respectively, MM_p, MM_{st} are the corresponding molecular masses and c_p, c_{st} are the concentrations. Errors have been calculated from the upper and the lower I(0) error limit estimated by the Guinier approximation. The shape of subunit α in solution was built by the program GASBOR (Svergun et al. 2001) as described in (Svergun et al. 2000).

Crystallization of subunit α of the *EC*F_1F_O ATP synthase

Sitting drops were prepared by 1:1 mixing of 12 mg/ml subunit α in buffer B (see above) with 2 M ammonium sulphate, 100 mM CAPS (N-cyclohexyl-3-aminopropanesulfonic acid), pH 10.5 and 200 mM lithium sulphate and incubated at 18 °C. Crystals were cryoprotected with 20% glycerol in crystallization buffer and flash frozen in liquid nitrogen. Data collection has been performed using a MAR research image-plate detector and Cu *Kα* rays in-house.

Determination of nucleotide binding properties via FCS

Fluorescence correlation spectroscopy (FCS) was performed at room temperature on a LSM 510 Meta/ConfoCor 3 (Zeiss, Jena, Germany) using the ATP- and ADP-analogues EDA-ATP ATTO-647N and EDA-ADP ATTO-647N (ATTO-TEC, Siegen, Germany). The temperature was adjusted to 25 °C in an incubation chamber (Zeiss). The 633 nm laser line of an HeNe633 laser (attenuated to 6 mW) was focused into the aqueous solution by a water immersion objective (40×/1,2 W Korr UL-VIS-IR, Zeiss). The experimental used buffer for subunit α consists of 50 mM Tris/HCl, pH 7.5 and 200 mM NaCl. FCS was measured in 15 µl droplets of the diluted fluorescent derivatives of ATP and ADP, which were placed on Nunc 8 well chambered cover glass. Before usage, the cover glasses were treated with 3% of gelatin, in order to prevent unspecific binding and removed by H_2O (Hunke et al. 2007). Solutions of Cyanine 5 (Cy5) in pure water (*Fluka*) were used as references for the calibration of the confocal microscope. The following filter sets were used: MBS: HFT 543/633, EF1: BP 655–710, EF: None, DBS: None. Out-of-focus fluorescence was rejected by a 90 µm pinhole in the detection pathway. The confocal detection volume was calculated to be approximately 0.32 fl at λ=655 nm at a numerical aperture (NA) of 1.2 variable concentrations of α and subunit B, respectively. Protein solutions were mixed with $MgCl_2$ and fluorescently labelled nucleotide, mixed, spun down rapidly to assure the volume, and the drop was instantaneously placed onto the glass slip. The drop was incubated for 3 min, which was monitored by FCS. The fluorescence autocorrelation functions were determined by measurements of about ten repetitions with 30 s each. To analyze the autocorrelation functions of fluorescent nucleotides bound to subunit α and subunit B, respectively, models with the diffusion time and the triplet state were used for fitting (FCS-LSM software, ConfoCor 3, Zeiss). The diffusion times of fluorescent nucleotides were measured independently and the determined values were kept fixed during the fitting of the FCS data. Based on this, the determination of the binding constants required only the calculation of the relative amounts of free nucleotides with the short diffusion time and of the bound nucleotides with the diffusion time of subunit α or subunit B. The calculations of the bound fractions and the dissociation constants were done by ConfoCor 3-software 4.2, Excel2003 and OriginPro 8 SR4.

Influence of effectors to the nucleotide binding to subunit α and subunit B by FCS

FCS was performed using the same instrument and nucleotide analogues as described above. NBD-Cl and DCCD were purchased at Sigma-Aldrich (St. Louis, MO, USA). These effectors were diluted in pure DMSO (dimethyl sulfoxide, Sigma-Aldrich). The DMSO content within the protein solution was at most 0.5%. The following filter sets were used: MBS: HFT 543/633, EF1: BP 655–710, EF: None, DBS: None. Out-of-focus fluorescence was rejected by a 90 μm pinhole in the detection pathway. The defined protein solution was pre-incubated with a fixed volume of the effector pre-dilutions (or buffer in case of the control) for 12 min and mixed at 7 °C. After the incubation time, $MgCl_2$ and Atto647N-labeled nucleotide were added, vortexed and spun down rapidly to assure the volume and placed the drop instantaneously onto the Nunc 8 well chambered cover glass. The drop was incubated on the blocked glass surface for 3 min. The fluorescence autocorrelation functions were determined by measurements of about ten repetitions with 30 s each. To analyze the autocorrelation functions of fluorescent nucleotides bound to subunit α and subunit B, respectively. The diffusion times of fluorescent nucleotides were measured independently and the determined values were kept fixed during the fitting of the FCS data. The calculation of the bound fraction was determined as described above. The IC_{50} value (concentration required for 50% inhibitory effect) was evaluated by OriginPro 8 SR4.

Results and discussion

Production and purification of a monodisperse subunit α

The SDS-PAGE of the produced recombinant subunit α of the $EC F_1F_O$ ATP synthase revealed a prominent band of 54 kDa which was found entirely within the soluble fraction. A Ni^{2+}-NTA resin column and an imidazole-gradient (25–300 mM) in buffer consisting of 50 mM Tris/HCl (pH 7.5) and 200 mM NaCl was used to separate subunit α from the main contaminating proteins. The protein, subunit α, eluting at 75–200 mM imidazole was collected and subsequently applied to a size exclusion chromatography (Superdex 75 HR 10/30 column). Analysis of the isolated protein by SDS-PAGE revealed the high purity of subunit α (Fig. 2a). The secondary structure of this subunit was determined from circular dichroism spectra, measured between 185 and 260 nm (Supplementary Fig. 1). The minima at 222 and 208 nm and the maximum at 192 nm indicate the presence of α-helical and β-sheet features in the protein and the secondary structure was calculated to be 45% α-helix and 33% random coil. The high purity and monodispersity of the protein is nicely indicated by small-angle X-ray scattering (SAXS) data and represented by the final composite scattering curve in Fig. 2a. The radius of gyration R_g and the maximum dimension D_{max} of subunit α are 2.76±0.1 nm and 9.66±0.1 nm, respectively (Fig. 2b). Comparison with the scattering from the reference solutions of BSA yields the estimate of molecular weight of 56±2 kDa, indicating that subunit α is monomeric at the concentrations used. The gross structure of subunit α was restored ab initio from the scattering pattern in Fig. 2a using the dummy residues modeling program GASBOR, which fitted well to the experimental data (Fig. 2a). The known atomic structure of subunit α from $EC F_1F_O$ ATP synthase (entry 1D8S (Hausrath et al. 1999)) was positioned inside the low resolution solution model. As shown in Fig. 2c this gross structure resembles very much the shape of the crystallographic model of subunit α from $EC F_1F_O$ ATP synthase, demonstrating the high quality of the purified recombinant protein. This is further supported by the fact that three dimensional crystals of α were grown with a size of 0.2×0.1×0.6 mm which diffract to 3.0 Å resolution (Fig. 2d).

Nucleotide-binding properties of subunit α

The monodisperse protein enabled us to study the ability of subunit α to bind nucleotides by fluorescence correlation spectroscopy using fluorescent ATP and ADP derivatives ATP ATTO-647N and ADP ATTO-647N, respectively. As a reference the mean count rate per Cyanine 5 (Cy5) fluorophore was determined to be 47.8 kHz (42.1 kHz). Compared to Cy5 the value of MgATP ATTO-647N was 70.5 kHz and 74.3 kHz for MgADP ATTO-647N alternatively. Fitting the autocorrelation functions resulted in characteristic times of diffusion τ_D=49.2 μs (54.1 μs) for Cy5, τ_D=71.7 μs for MgATP ATTO-647N and τ_D=66.9 μs for MgADP ATTO-647N. The autocorrelation curves in the absence and presence of increased concentrations of subunit α of the fluorescent ATP analogue for MgATP ATTO-647N are shown in Fig. 3a and for the appropriate ADP analogue in Fig. 3b. The increase of the mean diffusion time τ_D was due to the increase in the mass of the diffusing particle, when fluorescently labelled nucleotide is bound to α, which is apparent in the displayed autocorrelation curves with increased protein-concentrations from left to right. The determined bound fractions for rising concentrations of subunit α versus MgATP ATTO-647N are shown in Fig. 3c and the appropriate ADP analogue in Fig. 3d. Binding constants (K_d) of α of 1.6±0.3 μM of bound MgATP ATTO-647N (Fig. 3c) and 2.9 μM±0.2 of bound

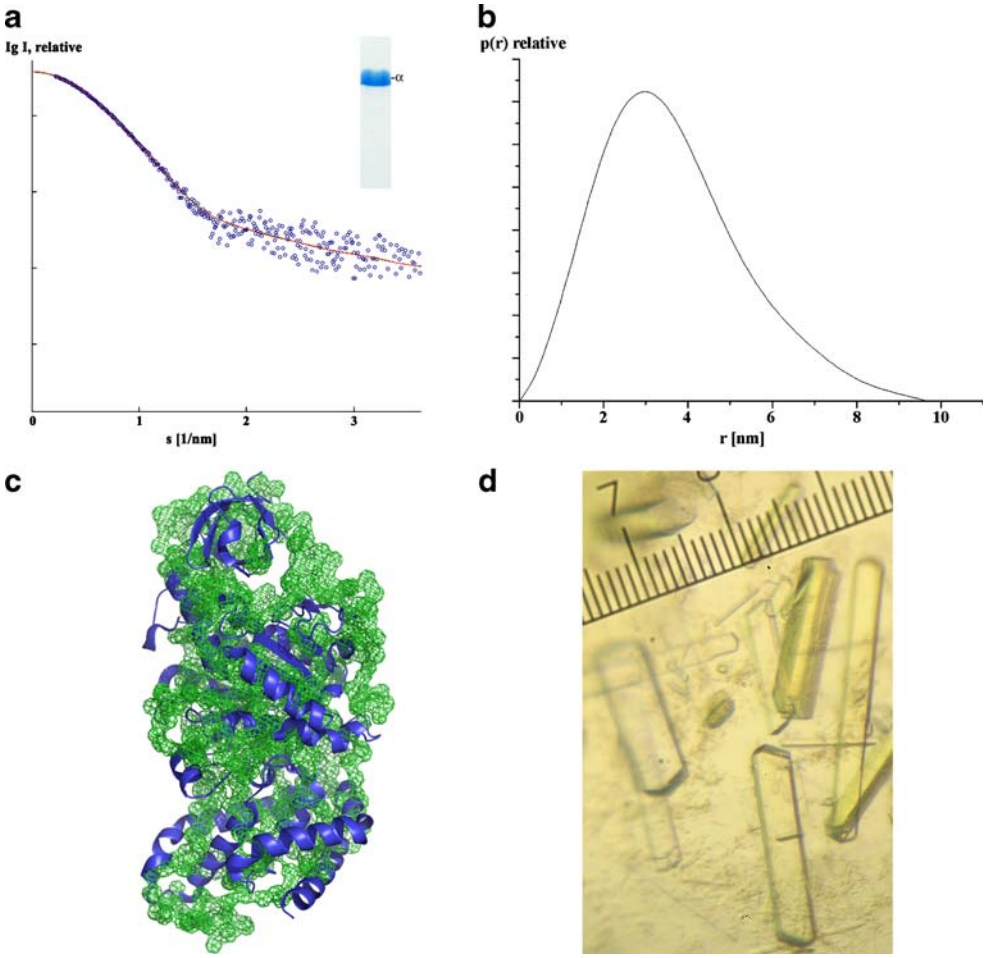

Fig. 2 (**a**) Experimental scattering curve (*white circle*) and scattering (*horizontal bar*) from ab initio model of subunit α of $EC F_1F_O$ ATP synthase. The insert represents an SDS-PAGE of the purified protein. (**b**) The distance distribution functions of subunit α. (**c**) Superposition of the GASBOR model of subunit α (*green*) with the crystallographic structure of the same protein (*blue* (1D8S, (Hausrath et al. 1999))). (**d**) 3D crystals of subunit α of $EC F_1F_O$ ATP synthase

MgADP ATTO-647N alternatively were determined (Fig. 3d and Table 1). By comparison, binding parameters for MgATP (25 μM) and MgADP (24 μM) have been described for all three α subunits in the $EC F_1$ ATPase using the intrinsic tryptophan signal of the genetically engineered residue R365 of subunit α (Weber et al. 1994a). The data confirm that the K_d values for ATP and ADP are in the same range of magnitude and that subunit α has no significant preference for the ATP- over the ADP analogue. The difference of binding strength between the recombinant α subunit and the mutated α subunits in the F_1 complex might be caused by the substitution of R365 to W in the mutant protein. Most recently we observed, that the exchange of R416 to W in the homologue subunit B of the A-ATP synthase from *M. mazei* Gö1 dropped the ATP- and ADP ATTO-647N binding compared to the wild-type (WT) protein (Kumar et al. 2009). At the same time, the crystallographic structure of both proteins revealed that the mutation of R416W abolished the existing salt bridge between amino acid Glu158 and R416, resulting in a reorientation of amino acid Glu158 (Kumar et al. 2009).

Influence of effectors to nucleotide-binding properties of subunit α

NBD-Cl reacts with the phenolic oxygen Y331 of the β_E subunit of the bovine mitochondrial F-ATP synthase (Andrews et al. 1984a,b; Sutton and Ferguson 1985; Haughton and Capaldi 1995; Orriss et al. 1998) and lies in a pocket, formed by amino acids of α_E (V334, S335, T340, I343) and β_E (V312, P313, A314 and D315), respectively. Two protein atoms, α_EI343 and β_ED315 are within 4Å of the NBD ring (Orriss et al. 1998). In order to prove, whether subunit α, comprising a part of the NBD-binding pocket, is also regulated by 4-Chloro-7-nitrobenzofurazan, the binding of subunit α to MgATP ATTO-647N and MgADP ATTO-647N in the presence of NBD-Cl has been studied by FCS. The plotted autocorrelation functions show a change of the diffusion time due to an increase of the concentration of NBD-Cl from right to left direction for MgATP ATTO-647N as well as for MgADP ATTO-647N (Fig. 4a–b). The calculated bound fraction for rising inhibitor concentrations were plotted to determine an effect to the nucleotide binding. The interac-

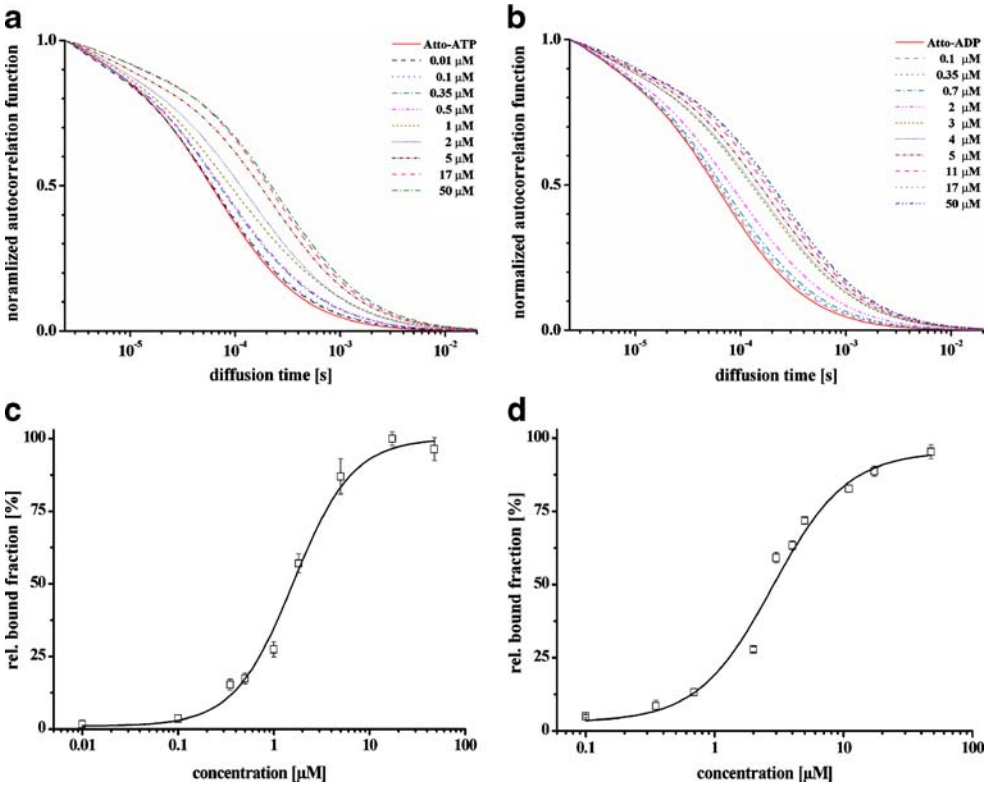

Fig. 3 Binding properties of subunit α of $EC F_1F_O$ ATP synthase to fluorescently labeled nucleotides. (**a**) Normalized autocorrelation functions of MgATP- and MgADP ATTO-647N (**b**) obtained by increasing the quantity of subunit α (increased protein concentration from *left to right*). (**c**) Binding of subunit α to MgATP ATTO-647N and (**d**) MgADP ATTO-647N displayed as relative bound fraction versus protein concentration. The best fits to titration *curves A and B* are shown as a non-linear, logistic curve fits

tion of MgATP ATTO-647N and MgADP ATTO-647N to subunit α showed an IC_{50} value of 51±3 μM (Fig. 4c, Table 1) and 55±3 μM with NBD-Cl (Table 1), respectively. From the crystallographic structure of the F_1-NBD complex, it has been predicted that the inhibitor might prevent subunit β_E from being changed into a nucleotide-binding state, a change that would otherwise be brought about by the rotation of the central γ subunit inside the enzyme (Orriss et al. 1998). Furthermore, Weber et al. (1994b) proposed that NBD-Cl prevents the binding of substrate to all three catalytic sites. The data presented demonstrate that besides the inhibitory effect in subunit β of F_1 ATPases, NBD-Cl changes the nucleotide-binding property of subunit α. This is in line with ATPase activity measurements of the $EC F_1$ ATPase mutant of subunit α S355A (S347A according to the *E. coli* residue numbering), in which the inhibitory effect of NBD-Cl in ATP hydrolysis was dropped by 20% (Li et al. 2009).

As N,N′-dicyclohexylcarbodiimide inhibits F_1 catalysis by binding into the α_{DP}-β_{DP} interface (Gibbons et al. 2000), the possible influence of DCCD to nucleotide-binding of subunit α has been tested. As demonstrated in Fig. 4d, even the increasing amounts to 2 mM of DCCD showed no influence in MgATP ATTO-647N or MgADP ATTO-647N binding (Table 1). These results support the specificity of the inhibitory effect of NBD-Cl in nucleotide-binding of subunit α and that the effect of DCCD inhibition in F_1 ATPase is due to covalent binding of DCCD to the catalytic β subunit.

Influence of effectors to nucleotide-binding property of subunit B

Previously, we observed that the recombinant subunit B of the *M. mazei* Gö1 A-ATP synthase binds MgATP ATTO-647N and MgADP ATTO-647N with K_d values of 22±

Table 1 Nucleotide binding constants of α and B in absence or presence of NBD-Cl and DCCD

	K_d (μM)	IC_{50} (inhibition due to NBD-Cl (μM))	IC_{50} (inhibition due to DCCD (μM))
ATP ATTO-647N binding to subunit α	1.6±0.3	51±3	No effect
ADP ATTO-647N binding to subunit α	2.9±0.2	55±3	No effect
ATP ATTO-647N binding to subunit B	22±3[a]	41±3	No effect
ADP ATTO-647N binding to subunit B	50±3 [a]	42±2	No effect

[a] Data were taken from Kumar et al. (2009)

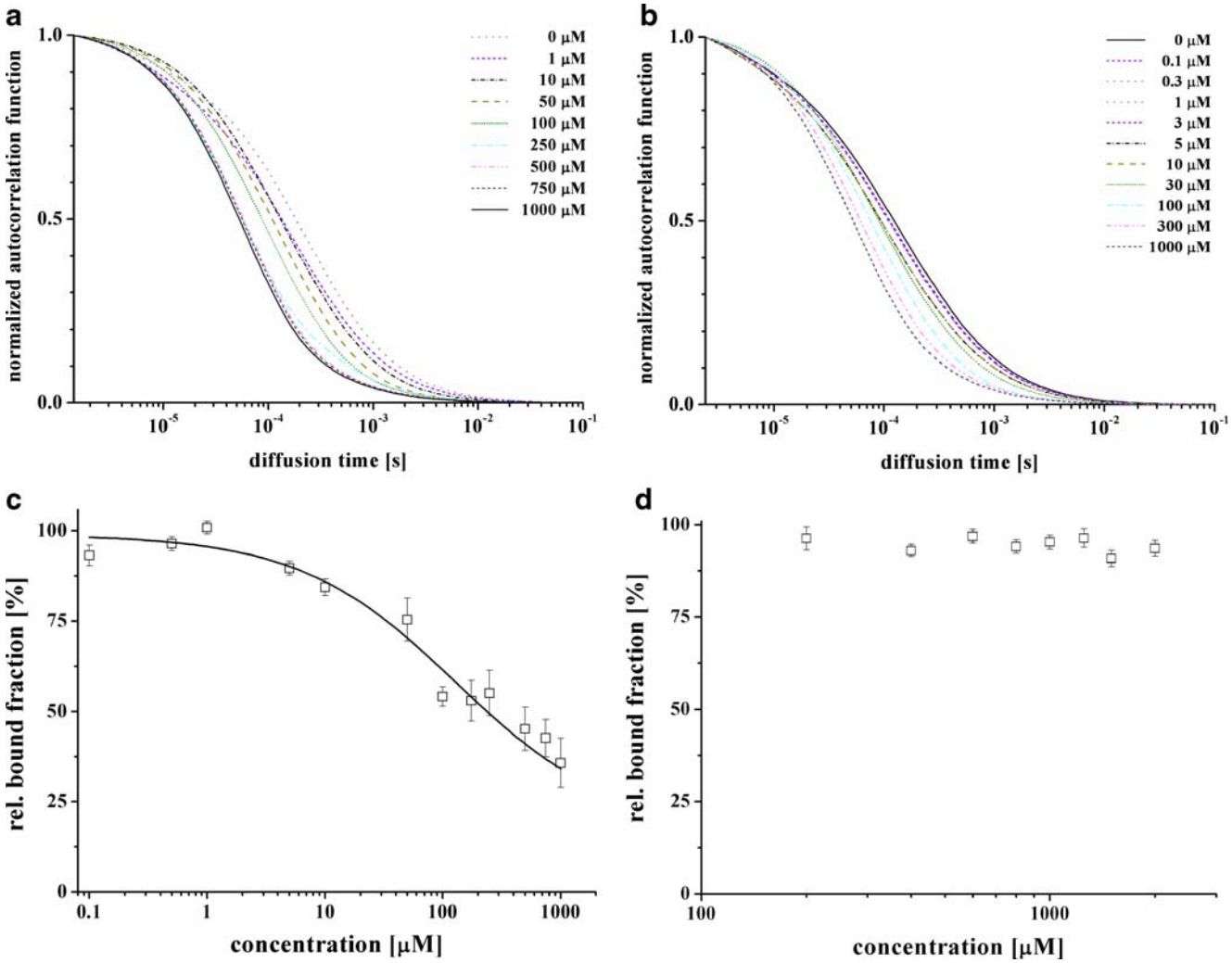

Fig. 4 Effector studies by fluorescence correlation spectroscopy. Effect of increased NBD-Cl concentration of MgATP (**a**) and MgADP ATTO-647N (**b**) bound to subunit α shown as normalized autocorrelation functions (increased effector concentration from *right to left*). (**c**) Influence of NBD-Cl and DCCD (**d**) to MgATP ATTO-647N binding properties of subunit α. The best fits at titration *curves A and B* are shown as a pharmacological dose-response curve with variable Hill slope

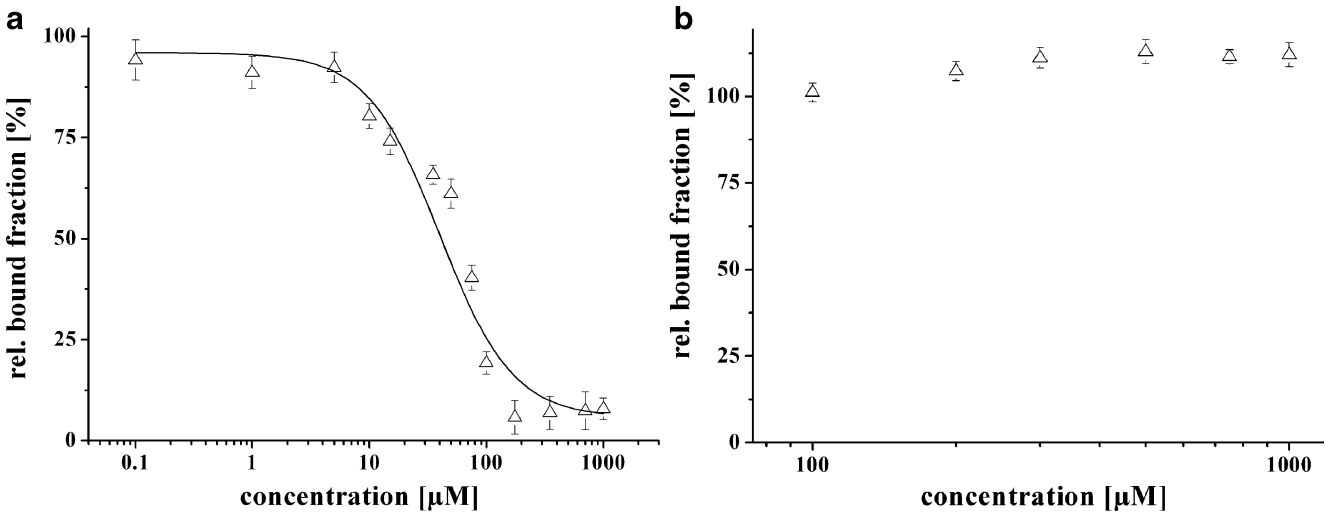

Fig. 5 Influence of effectors to MgATP ATTO-647N binding properties of subunit B of A-ATP synthase from *M. mazei* Gö1 shown as bound fraction versus effector concentration. NBD-Cl (**a**) and DCCD (**b**) titration to subunit B versus MgATP ATTO-647N

3 μM and 50±3 μM, respectively, indicating a preference for the ATP- over the ADP analogue (Kumar et al. 2009, Table 1), which might be important for regulatory or mechanistic events in the A–B interface of the A_1 headpiece. As subunit B is proposed to be a homologue subunit of α (Hilario and Gogarten 1998), NBD-Cl has been tested to be a potent inhibitor of nucleotide-binding in subunit B. The effect of NBD-Cl to the binding of subunit B of the A_1A_O ATP synthase from *M. mazei* Gö1 to MgATP ATTO-647N is shown in Fig. 5a. The calculated bound fraction for rising inhibitor concentrations were plotted to determine the effect to the nucleotide binding (Fig. 5a). An IC_{50} value of 41±9 μM in the case of NBD-Cl effecting the interaction of MgATP ATTO-647N to subunit B was determined (see Table 1). In comparison, NBD-Cl inhibits MgADP ATTO-647N in subunit B by an IC_{50} value of 42±2 μM (Table 1). In contrast, DCCD showed no influence in the concentration range used, neither in case of MgATP ATTO-647N nor MgADP ATTO-647N (Fig. 5b, Table 1), underlining the specificity of the NBD-Cl effect in nucleotide-binding of subunit B. The availability of the X-ray structure of subunit B of *M. mazei* Gö1 A-ATP synthase (Schäfer et al. 2006) allows one to discuss the possible amino acids forming an NBD-binding pocket and shows that the residues T340, I343 and F351, contributing to the NBD-pocket in subunit α, are replaced by the homologue/identical amino acids S318, I321 and V327 in subunit B and therefore, being possible candidates to form the binding-pocket for NBD-Cl in subunit B. Recently, crystallographic structures showed that the subunit B mutant R416W trap ATP in two transition positions and therefore allowed us to propose a trail that the ATP takes on its way to the final binding pocket (Kumar et al. 2009; Manimekalai et al. 2009). One of the trapped ATP position is similar to one of the binding region of the antibiotic efrapeptin C, a potent inhibitor of ATP synthases in mitochondria, some bacterial species (Jost et al. 2007; Abrahams et al. 1996) and the reconstituted A_3B_3-subcomplex of *M. mazei* Gö1 A-ATP synthase (Kumar et al. 2009). From these structural and additional functional studies, it has been predicted that the binding of the antibiotic efrapeptin C blocks the transition ATP binding site of subunit B. As shown for F_1 ATPase, the NBD-Cl binding pocket is located in the interface of the nucleotide-free subunits α and β which is 13 Å away from the phosphate-loop (Orriss et al. 1998). The inhibition of NBD-Cl to the ATP/ADP-binding in subunit α and B, respectively, indicates, that the effect(s) of NBD-Cl is not only limited to β subunit and the mechanism of ATP hydrolysis and/or synthesis in the case of F-ATP synthases, but includes also the binding of nucleotides in the major subunits α and B, which together with the subunits β and A form the catalytic unit in the biological motor proteins F- and A-ATP synthase.

Since ATP synthases have been suggested as a good molecular target for inhibitors in the treatment of various diseases and the regulation of energy metabolism (Hong and Pedersen 2008), accumulation of knowledge about the mechanistic effect of inhibitors is essential for generating concepts for new agents or to modify the structural and thereby the chemical traits of potent inhibitors. The data presented give insight into the interaction of the agent NBD-Cl in the inhibition of energy producers F-ATP synthase and A-ATP synthase and may represent a new target area for modified or novel classes of ATP synthase agents.

Acknowledgments We thank Dr. A. Balakrishna and A. Kumar for crystallographic data collection and isolation of subunit B from *M. mazei* Gö1, respectively. This research and the fellowship for Vikeramjeet S. Tadwal were supported by a grant from the Ministry of Education, Singapore (ARC 6/06 and RG144/06).

References

Abrahams JP, Buchanan SK, van Raau MJ, Fearnley IM, Leslie AGW, Walker JE (1996) Proc Natl Acad Sci U S A 93:9420–9424
Andrews WW, Hill FC, Allison WS (1984a) J Biol Chem 259:8219–8225
Andrews WW, Hill FC, Allison WS (1984b) J Biol Chem 259:14378–14382
Bernal RA, Stock D (2004) Structure 12:1789–1798
Biuković G, Rössle M, Gayen S, Mu Y, Grüber G (2007) Biochemistry 46:2070–2078
Boulin CJ, Kempf R, Koch MHJ, McLaughlin SM (1986) Nucl Instrum Methods A249:399–407
Coskun Ü, Radermacher M, Müller V, Ruiz T, Grüber G (2004a) J Biol Chem 279:22759–22764
Coskun Ü, Chaban YL, Lingl A, Müller V, Keegstra W, Boekema EJ, Grüber G (2004b) J Biol Chem 279:38644–38648
Cross RL, Müller V (2004) FEBS Lett 576:1–4
Deppenmeier U, Müller V (2008) Results Probl Cell Differ 45:123–152
Gibbons C, Montgomery MG, Leslie AG, Walker JE (2000) Nat Struct Biol 7:1055–1061
Gledhill JR, Walker JE (2006) Biochem Soc Trans 34:989–992
Grüber G, Capaldi RA (1996) J Biol Chem 271:32623–32628
Grüber G, Marshansky V (2008) BioEssays 30:1096–1109
Grüber G, Godovac-Zimmermann J, Link TA, Coskun Ü, Rizzo VF, Betz C, Bailer S (2002) Biochem Biophys Res Commun 298:383–391
Guinier A, Fournet G (1955) Small angle scattering of x-rays. Wiley, New York
Haughton MA, Capaldi RA (1995) J Biol Chem 270:20568–20574
Hausrath AC, Grüber G, Matthews BW, Capaldi RA (1999) Proc Natl Acad Sci U S A 96:13697–13702
Hilario E, Gogarten JP (1998) J Mol Evol 46:703–715
Hong S, Pedersen PL (2008) Microbiol Mol Biol Rev 72:590–641
Hunke C, Chen W-J, Schäfer H-J, Grüber G (2007) Protein Expr Purif 53:378–383
Jost M, Weigelt S, Huber T, Majer Z, Greie J-C, Altendorf K, Sewald N (2007) Chem Biodiversity 4:1170–1182
Kumar A, Manimekalai MSS, Balakrishna AM, Hunke C, Weigelt S, Sewald N, Grüber G (2009) Proteins: Struct, Funct, Bioinf 75:807–819

Laemmli UK (1970) Nature 227:680–685
Leslie AGW, Walker JE (2000) Philos Trans R Soc Lond B 355:465–471
Li W, Brudecki LE, Senior AE, Ahmad Z (2009) J Biol Chem 284:10747–10754
Lolkema JS, Chaban Y, Boekema EJ (2003) Bioenerg Biomembr 35:323–336
Manimekalai MSS, Kumar A, Balakrishna A, Grüber G (2009) J Struct Biol 166:39–45
Nelson N (1992) Biochim Biophys Acta 1100:109–124
Orriss GL, Leslie AGW, Braig K, Walker JE (1998) Structure 6:831–837
Pedersen P, Ko YH, Hong S (2000) J Bioenerg Biomembr 32:325–332
Roessle MW, Klaering R, Ristau U, Robrahn B, Jahn D, Gehrmann T, Konarev PV, Round A, Fiedler S, Hermes S, Svergun DI (2007) J Appl Crystallogr 40:190–194
Round AR, Franke D, Moritz S, Huchler R, Fritsche M, Malthan D, Klaering R, Svergun DI, Roessle M (2008) J Appl Crystallogr 41:913–917
Schäfer I, Bailer SM, Düser MG, Börsch M, Ricardo AB, Stock D, Grüber G (2006) J Mol Biol 358:725–740
Sutton R, Ferguson SJ (1985) Eur J Biochem 148:551–554
Svergun DI (1993) J Appl Crystallogr 26:258–267
Svergun DI, Bećirević A, Schrempf H, Koch MHJ, Grüber G (2000) Biochemistry 39:10677–10683
Svergun DI, Petoukhov MV, Koch MHJ (2001) Biophys J 80:2946–2953
Vonck J, Pisa KY, Morgner N, Brutschy B, Müller V (2009) J Biol Chem 284:10110–10119
Walker JE, Dickson VK (2006) Biochim Biophys Acta 1757:286–296
Weber J, Wilke-Mounts S, Grell E, Senior AE (1994a) J Biol Chem 269:11261–11268
Weber J, Wilke-Mounts S, Senior AE (1994b) J Biol Chem 269:20462–20467